Insights into uptake, distribution, and efflux of arsenite associated with nano-TiO2 in determining its toxicity on Daphnia magna

Journal:	*Environmental Science: Nano*
Manuscript ID	EN-ART-12-2019-001453
Article Type:	Paper

SCHOLARONE™
Manuscripts

Environmental Science: Nano

Environmental significance statement

Only limited information is available on the effects of titanium dioxide nanoparticles (nano-TiO_2) on arsenite (As(III)) accumulation and its ensuing toxicity within aquatic organisms. It is, however, of particular importance to understand the appropriate exposure levels and exposure times to better interpret their ecotoxicological effects while utilizing subcellular fractions. Results from this study showed that as a carrier nano-TiO_2 increased As(III) accumulation in *Daphnia magna* but not its subsequent level of toxicity. Regardless of exposure time or level, the subcellular distribution of As(III) can itself explain the toxic effects on daphnids. Furthermore, direct and reproduction efflux were found to be the two main pathways used to expel accumulated As and Ti from daphnids. The significance of our findings can be used to understand the ecological risks of nano-TiO_2 and its associative role in heavy metal contamination.

Insights into uptake, distribution, and efflux of arsenite associated with nano-TiO$_2$ in determining its toxicity on *Daphnia magna*

Zhuanxi Luo[1,2*], Zhenhong Wang[3], Baoshan Xing[4]

1. College of Chemical Engineering and Fujian Provincial Key Laboratory of Biochemical Technology, Huaqiao University, Xiamen 361021, China

2. Key Laboratory of Urban Environment and Health, Institute of Urban Environment, Chinese Academy of Sciences, Xiamen 361021, China

3. College of Chemistry and Environment and Fujian Province Key Laboratory of Modern Analytical Science and Separation Technology, Minnan Normal University, Zhangzhou 363000, China

4. Stockbridge School of Agriculture, University of Massachusetts, Amherst, Massachusetts 01003, United States of America

* Corresponding author;

Email address: zxluoire@163.com (Z. Luo)

Abstract: Only limited information is available on the effects of titanium dioxide nanoparticles (nano-TiO$_2$) on arsenite (*As*(III)) accumulation and its ensuing associated toxicity in aquatic organisms. This study characterized *As*(III) uptake, spatial and subcellular distribution, and efflux under different exposure treatments and its toxicity on *Daphnia magna* in the presence of nano-TiO$_2$. Results showed that accumulated arsenic (*As*) content was significantly correlated to the corresponding accumulated titanium (Ti) content, implying that nano-TiO$_2$ as a carrier increased *As*(III) accumulation in *D. magna*. Additionally, a significant spatial correlation between *As* and Ti accumulation further confirmed the "carrier" role of nano-TiO$_2$, while this role weakened under higher *As*(III) exposure levels due to its elevated toxicity and its limited adsorption capacity onto nano-TiO$_2$. Also, despite an increase in *As*(III) accumulation, nano-TiO$_2$ decreased *D. magna* toxicity. Specifically, the

1

24-h As(III) EC_{50} increased from 2.53 mg As/L to 2.97 mg As/L while nano-TiO_2 increased from 2 to 20 mg Ti/L. This reduction in toxicity resulted from the accumulation of most As in biologically detoxified metals (BDM) and cellular debris as detoxified fractions. Moreover, the similarity in As and Ti subcellular distribution was clearly observed between 6 h and 24 h exposure and between 75 μg As/L and EC_{50} exposure levels of $As(III)$. Therefore, regardless of exposure time or exposure As(III) level, the subcellular distribution of As can itself explain its toxic effects on daphnids resulting from As(III) stress associated with nano-TiO_2. Interestingly, elevated nano-TiO_2 produced lower As efflux from daphnids, which showed that nano-TiO_2 still sequestered some As within this organism. Lastly, direct and reproduction efflux were the two main pathways that daphnids used to eliminate accumulated As and Ti. These findings can help us to better understand the ecological risks of nano-TiO_2 and its co-existing contaminants in the environment.

Keywords: arsenic; nanomaterials; transport; accumulation; subcellular fractions

1 Introduction

Arsenic (As), a toxic, non-essential metalloid, have been listed in the priority list of hazardous substances by the Agency for Toxic Substances and Disease Registry (ATSDR) due to its high toxicity at global scale[1, 2]. Both the anthropogenic sources and naturally occurring sources can contribute to As contamination in the environment, depending on its cases and places[3, 4]. Moreover, As and its associative compounds in the environment constantly transform into different forms and can be transported into different media, making it difficult to be eliminated over a long period of time[5, 6]. By either acute or chronic exposure, it will eventually harm to both ecosystems and human health[7, 8]. Accordingly, the World Health Organization (WHO) set the total arsenic (TAs) standard of drinking water at 10 μg/L. Similarly, in 2006 China also improved its TAs standard for drinking water, namely, reducing it from 50 μg/L to 10 μg/L. Michael reported that about 140 million people worldwide are at risk for arsenic exposure through drinking water[9]. They also estimated that more than 19 million Chinese may be drinking water above the WHO guideline.

1
2
3
4
5
6
7
8
9
10
11
12
13
14
15
16
17
18
19
20
21
22
23
24
25
26
27
28
29
30
31
32
33
34
35
36
37
38
39
40
41
42
43
44
45
46
47
48
49
50
51
52
53
54
55
56
57
58
59
60

Furthermore, *As* mainly exists in its trivalent state (i.e., arsenite *As*(III)) and its pentavalent state (i.e., arsenate *As*(V)) in aquatic environments, but *As*(III) is more toxic than *As*(V), being more soluble and mobile in the environment[10]. Accordingly, more attention must be paid to the ecological effects of *As*(III).

Titanium dioxide nanoparticles (nano-TiO$_2$) are widely used in biomedicine, information technology, catalyst and sewage treatments, etc., due to their unique physical and chemical properties[11-13]. Consequently, during the process of production, storage, use, and disposal, nano-TiO$_2$ inevitably enters the water environment. Nano-TiO$_2$ has a larger specific surface area with a strong adsorption ability, which allows it to strongly adsorb pollutants within the environment[14, 15]. This higher adsorption ability effectuates changes in the environmental behavior of adsorbed pollutants, thus changing their potential biological effects[16]. For example, Rosenfeldt et al.[17] found that nano-TiO$_2$ increased silver (Ag) toxicity in daphnids and as a carrier increased its overall accumulation within these organisms. Fan et al.[18] also found that nano-TiO$_2$ increased copper (Cu) accumulation in daphnids through its adsorption ability. Moreover, Yang et al.[19] reported that nano-TiO$_2$ can act as a carrier of cadmium (Cd), influencing its toxicity and accumulation in aquatic organisms. Yan et al. [20] demonstrated that *As*(V) uptake was significantly facilitated by nano-TiO$_2$ in the nauplii of *Artemia salina*. Furthermore, nano-TiO$_2$ and *As*(III) co-occur in the water environment, and the adsorption of *As*(III) onto nano-TiO$_2$ acting as a carrier impacts *As*(III) accumulation within organisms and their ensuing level of toxicity[17, 21]. Similarly, our previous study found that 20 mg/L of nano-TiO$_2$ increased *As*(V) accumulation and its toxicity in *Daphnia magna*[21]. Although previous studies have investigated the accumulation of heavy metals and associative toxicity in aquatic organisms influenced by the presence of nano-TiO$_2$, the effects of nano-TiO$_2$ on *As*(III) accumulation and its associative toxicity within aquatic organisms are relatively scarce.

Additionally, investigating the distribution of elements in organisms helps to identify accumulation and detoxification mechanisms of heavy metals[22, 23]. Furthermore, metal detoxification methods used by daphnids include binding metals with metallothionein, generating precipitation with insoluble mineral particles, or entering lysosomes or membrane vesicles, trapping them before removing them through metabolic processes. Another detoxification strategy of daphnids is to

increase the release ratio of metals to expel any excess[24]. The subcellular distribution of metals can respond dynamically to changes in exposure conditions and environmental factors[25]. Therefore, a subcellular distribution model can better reflect the accumulation patterns and detoxification strategies adopted by organisms in the face of metal exposure under different environmental conditions, and such a model can also better explain and predict metal bioavailability, toxicity, and transmission in the food chain[19, 20]. In our previous study, we applied subcellular compartmentalization (based on subcellular fractions) as metal-sensitive fractions (MSF), biologically detoxified metals (BDM), and cellular debris at a lower 3 h As(V) exposure treatment to interpret the ecotoxicological effects of As(V) on $D. magna$ in the presence of nano-TiO$_2$[21, 26]. However, subcellular compartmentalization could be dynamically affected by different pollutant exposure levels as well as corresponding times of exposure, which could conduce different overall subcellular distribution results. Therefore, the effects of pollutant exposure levels and their corresponding exposure times in interpreting ecotoxicology remain unclear. It is thus necessary to better understand the appropriate exposure levels and exposure times to correctly interpret ecotoxicological effects while utilizing subcellular fractions.

$Daphnia magna$ is a planktonic crustacean, widely distributed in freshwater environments. As a common and standard aquatic test organism, $D. magna$ (a zooplankton) is widely used in toxicology experiments. Affiliated with the second trophic level of the food chain, zooplankton can convert plant-based nutrition to animal nutrition, thereby occupying an important position within the food chain. The accumulation of heavy metals in $D. magna$ could, however, be potentially harmful to human health through heavy metal transfer across the food chain. Accordingly, in this study we investigated the uptake, distribution, and efflux of As(III) in $D. magna$ as well as the ensuing level of As(III) toxicity influenced by nano-TiO$_2$. In order to validate the appropriate exposure level and exposure time from which to interpret their corresponding toxicological effects, we selected two As(III) toxicity treatment levels of 75 μg/L (lower) and EC$_{50}$ (higher) and two exposure time treatments of 6 h and 24 h to explore As(III) uptake and distribution in $D. magna$ associated with

different levels of nano-TiO$_2$. Our findings could potentially be of great significance in understanding the ecological risks of nano-TiO$_2$ and its associative heavy metal contamination.

2 Materials and Methods

2.1 Model species (*Daphnia magna*) and stock suspension preparation

We continuously cultured *D. magna* specimens in our laboratory, which we obtained from Sun Yat-sen University (Guangzhou, China). *Scenedesmus obliquus* specimens were used as a daily food source at a density of 5×10^5 cells/mL. The culture medium (i.e., simplified Elendt M7 medium; SM7) was changed every 2 d. The culture was maintained at a constant temperature (22 °C ± 2 °C) and light intensity (3500 lx) under a natural light-dark (16 h : 8 h) cycle.

Anatase-type nano-TiO$_2$ (CAS No. 1317-70-0) was purchased from the Sigma-Aldrich Chemicals Co. (St. Louis, MO, USA), which they claimed to have an average surface area of 50 m^2/g and an average primary particle size of 25 nm. A nano-TiO$_2$ stock solution of 1.0 g Ti/L was prepared by dispersing the nanoparticles in ultrapure water (MilliporeSigma, Billerica, MA, USA) under 10 min sonication (50 W/L at 40 kHz) prior to its application. Using the dynamic light scattering (DLS) technique immediately afterwards to determine the average particle size, we ascertained that the dimension of the nano-TiO$_2$ specimens was 70.5 ± 11.2 nm [21]. At the same time, using a scanning electron microscope (SEM S-4800, Hitachi, Japan; Fig. S1), the aggregation size of nano-TiO$_2$ was determined to be from a few hundred nanometers (nm) to several microns (μm) in diameter in the SM7 medium. Furthermore, NaAsO$_2$·12H$_2$O (Sigma-Aldrich Chemicals Co.) was used for the preparation of the *As*(III) stock solutions at a concentration of 100 μM. The stock solutions were stored at 4 °C under darkened conditions until utilized. Other guaranteed-grade chemical reagents were also utilized.

2.2 Arsenite adsorption onto nano-TiO$_2$

To determine *As*(III) adsorption onto nano-TiO$_2$, we prepared nano-TiO$_2$ suspensions

of 2 and 20 mg Ti/L (final concentration) in 50 mL centrifuge tubes. We then added 75 μg/L of *As*(III) to the nano-TiO$_2$ suspensions. The final mixed nano-TiO$_2$ suspension volume including *As*(III) was 40 mL. In order to prevent the occurrence of *As*(III) photo-oxidation, all experiments were conducted in the dark. Three replicates were established for each treatment. These mixtures were then oscillated at the speed of 180 r/min and at a temperature of 25 °C for 24 h. According to our previous study[21], 1.5 mL of the nano-TiO$_2$ suspensions was collected at 0, 0.5, 1, 2, 3, 12, and 24 h from the above mentioned oscillated mixtures. These samples were then centrifuged twice for 10 min under 12 000 g. 1 mL of the supernatant was then collected to ascertain T*As* and total titanium (wherein greater than 95% nano-TiO$_2$ was removed during the centrifugal process) using inductively coupled plasma mass spectrometry (ICP-MS, Agilent Technologies 7500a).

2.3 Acute toxicity

We conducted a 24 h toxicity test based on the modified Organization for Economic Co-operation and Development (OECD) standard procedure. Briefly, we used a series of nine *As*(III) concentrations in total, namely, 0, 5, 10, 20, 25, 30, 35, 40, and 50 μM associated with three nano-TiO$_2$ levels (0.0, 2.0, and 20.0 mg Ti/L) in the selected media. At the same time, *As*(III) and nano-TiO$_2$ toxicity tests were separately conducted as controls to assess the individual effects of nano-TiO$_2$ and *As*(III) toxicity. For each treatment, we placed 10 neonates (from 6 to 24-h old) of similar size from a designated brood into 200 mL glass beakers, which were continuously cultured (producing greater than three generations). Finally, we assessed the mortality of individuals in each beaker. Herein, *D. magna* specimens that were not observed to swim after gentle agitation for 15 s were considered expired. All experiments were conducted in triplicate under darkened conditions. We calculated 24-h EC$_{50}$ values as well as their associated 95% confidence intervals (95% CI) using a graphical probability unit method (as shown in Table S1). Specifically, 24-h EC$_{50}$ values under three nano-TiO$_2$ levels of 0, 2, and 20 mg Ti/L were thus calculated at 0.93, 2.53, 2.97 mg *As*/L, respectively. In the following experiments, we then used the above-calculated 24-h EC$_{50}$ values (i.e., 0.93, 2.53, and 2.97 mg *As*/L) to establish one

of the exposed *As*(III) levels associated with the corresponding nano-TiO$_2$ levels (i.e., 0, 2, and 20 mg/L, respectively).

2.4 Arsenic accumulation in *Daphnia magna*

During these experiments, *D. magna* specimens were exposed to *As*(III) adsorbed onto either low (2.0 mg Ti/L) or high (20.0 mg Ti/L) nano-TiO$_2$ concentrations. The nano-TiO$_2$ test solutions were prepared at three final levels, namely, 0 (control), 2, and 20 mg Ti/L in beakers by diluting the nano-TiO$_2$ stock solutions. The final *As*(III) exposure concentration was 75 μg/L, including its corresponding EC$_{50}$ value levels. We employed three replicates for each treatment which contained 250 7-d old daphnid specimens of similar size (1 individual/10 mL). We first removed daphnids to allow for gut evacuation over a 3-h period in SM7 media devoid of food particles. We then collected 10 daphnids at 20, 40, 60, 120, 180, 360, 720, and 1440 min from each beaker under the three nano-TiO$_2$ exposure levels for *As* and Ti content analysis. At the same time, we collected 5 daphnids at 360 min (6 h) from each of the three nanoparticles exposure beakers under the 75 μg/L arsenite treatment for spatial analysis. Similarly, 100 daphnids at 360 min and 1440 min (24 h) were collected under all treatments for subcellular distribution analysis. At 1440 min, we collected 120 daphnids for our *As*(III) and nano-TiO$_2$ efflux experiments. We washed the collected daphnids for a few seconds in ultrapure water to remove the circumambient exposure media. Following this, a number of 0.1 M potassium phosphate buffers (pH 7.0) were used to remove external *As*. To analyze the body burden of *As* and Ti in daphnids, sampled daphnid specimens were treated as per our previous method[21]. Briefly, after quickly washing daphnids in ultrapure water to remove the potassium phosphate buffer, specimens were placed into bullet vials for freeze-drying. After weighing daphnids and then adding 50 μL nitric acid (HNO$_3$) (69%) and (after 12 h) 50 μL hydrofluoric acid (HF) (40%), we dissolved daphnids after 4 h applying intermittent microwave digestion (4 min at 100 W, 3 min at 180 W, 2 min at 180 W, 2 min at 300 W, 2 min at 300 W, and 2 min at 450 W), after which the samples were diluted to 1–2% HNO$_3$. Finally, we used ICP-MS to measure T*As* and Total Ti concentrations (Agilent 7500a)[21].

2.5 Spatial and subcellular distribution

To measure spatial distribution, samples were oven-dried at 60 °C to obtain a constant weight. Additionally, in order to confirm whether nano-TiO$_2$ was able to transport *As*(III) to daphnid tissues (i.e., not only into their intestinal tracts), we incised extra tissue removed from intestinal tracts using an operating scalpel. According to our previous method[21], the spatial distribution of *As* and Ti in daphnids and tissues was determined using laser ablation inductively coupled plasma mass spectrometry (LA-ICP-MS) (GeoLas 2005 system, ICP-MS, Agilent 7500a).

Furthermore, we determined subcellular partitioning of T*As* and Ti in the body tissues of *D. magna* using our previously modified differential centrifugation method[21]. We obtained a total of five different fractions, including cellular debris (containing cell membranes), organelles (containing nuclear, mitochondrial, microsomes, and lysosomes), heat-denatured protein (HDP; containing enzymes), heat-stable protein (HSP; or metallothionein-like proteins), and metal-rich granules (MRG). We separately assayed all T*As* and Ti fraction concentrations to allow for the estimation of *As* and nano-TiO$_2$ subcellular partitioning. Results were expressed in mg (dry weight) per individual. The subcellular fraction rate of recovery was approximately from 86% to 105%. MRG and HDP are generally classified as BDMs in living organisms, while organelles and HSP are considered as MSFs. Accordingly, we used the two combined BDM and MSF fractions to explain *As*(III) toxicity in daphnids associated with nano-TiO$_2$.

2.6 Arsenic and nano-TiO$_2$ elimination

The above mentioned (see section 2.4) daphnid samples were placed into purified SM7 media devoid of *As*(III) and nano-TiO$_2$ to investigate the elimination of *As*(III) and nano-TiO$_2$ from *D. magna*. Briefly, 7-d old daphnid samples as well as one-day old pregnant specimens fully inoculated with sperm were exposed for 6 h (to reach an accumulation equilibrium) to 75 μg/L *As*(III) along with nano-TiO$_2$ of 0, 2, and 20 mg/L in SM7. After exposure, all daphnid specimens were washed using the above mentioned potassium phosphate buffer to remove external *As* and nano-TiO$_2$. These daphnid specimens were then placed into purified SM7 for 24 h to determine *As*(III)

and nano-TiO$_2$ elimination rates. At the same time, sperm samples were carefully collected and washed in the above mentioned potassium phosphate buffer for further *As* and Ti detection, which is considered "reproduction" efflux from daphnia. During the elimination process, every 15 daphnid specimen was collected at 0, 1, 3, 6, 12, and 24 h for rinsing with ultrapure water and then freeze-dried for further *As* and Ti detection. Additionally, water samples from the above mentioned SM7 elimination solutions were used to detect *As* and Ti for "direct" efflux from daphnid samples. Following this, we determined the molting efflux of *As* and Ti to be the subtracted amount from the corresponding content in daphnids at 0 h between direct efflux and reproduction efflux. Specifically, we applied our previous methods to detect *As* and Ti in daphnids, solutions, and sperm using ICP-MS [21].

2.7 Statistical Analysis

SPSS 12.0 was used to conduct statistical analysis on the data. Data are shown as means with standard deviations (SD). Differences within treatment groups were evaluated using two-way analysis of variance (ANOVA) with the least significant difference (LSD) range test. Significant differences were considered acceptable at *P*<0.05.

3 Results and Discussion

3.1 Arsenite adsorption onto TiO$_2$ nanoparticles

The adsorption of *As*(III) onto two different nano-TiO$_2$ concentration levels (i.e., 2 and 20 mg/L) achieved equilibrium within 30 min, wherein their adsorption rates were 31.38% and 51.84%, respectively (Fig. S2). This showed that *As*(III) rapidly adsorbed onto nano-TiO$_2$ in our test solutions. Additionally, the *As*(III) adsorption rate onto nano-TiO$_2$ was far lower than the *As*(V) adsorption rate under the same conditions (i.e., 56% and 98%, respectively)[21]. The co-contaminant adsorption rate onto nano-TiO$_2$ is dependent on its physical and chemical properties as well as the surrounding environment. Characteristics of nano-TiO$_2$ are its small particle size, its large surface area, its substantial atomics on the surface, and empty bonds, leading to

the faster, relatively stronger adsorption capacity of As(III)[14]. Moreover, As adsorption onto nano-TiO$_2$ is largely reliant on the pH level of the As medium. Previous studies showed that pH strongly influences the adsorption of As(III) onto nano-TiO$_2$, which increases with increasing pH level[27, 28]. In this study, the pH level in the test medium was less than 9.1. Under this condition, As(III) in the test solution was primarily characterized as a neutral (non-ionized) As species (i.e., As(OH)$_3$ and AsO(OH)$^{2-}$), and the nano-TiO$_2$ surface was negatively charged, making the adsorption capacity of As(III) onto nano-TiO$_2$ lower than As(V)[29].

3.2 Titanium dioxide nanoparticles influence on arsenite uptake

Changes in As and Ti accumulation in $D. magna$ under the two As(III) exposure levels exhibited similar trends, which were strongly influenced by nano-TiO$_2$ (Fig. 1). Specifically, nano-TiO$_2$ significantly increased the body burden of As in $D. magna$ ($P<0.05$), suggesting that nano-TiO$_2$ as a carrier of As(III) increased As accumulation in this organism[17]. For the lower 75 µg/L As(III) exposure treatment, As content in $D. magna$ was 126.67 µg/g and 165.36 µg/g with the addition of 2 and 20 mg/L nano-TiO$_2$, respectively, which was greater by a factor of 2.9 and 3.8, respectively, compared to the control (Fig. 1 A). By contrast, for the higher EC$_{50}$ As(III) exposure treatment, As content in $D. magna$ was 160.47 and 218.01 µg/g with the addition of 2 and 20 mg/L nano-TiO$_2$, respectively, which was greater by a factor of 1.8 and 2.5, respectively, compared to the control (Fig. 1 B). Additionally, Ti accumulation in daphnids under the two As exposure levels was 2.5 and 5.74 mg/g (Fig. 1 C) and 1.57 and 3.47 mg/g (Fig. 2 D) for the 2 and 20 mg/L nano-TiO$_2$ treatments, respectively. It was therefore obvious that Ti content in $D. magna$ increased with increasing nano-TiO$_2$ levels but decreased with increasing As exposure levels (Fig. 1). This suggested that an increase in exposure As could weaken the ingestive ability of daphnids, subsequently decreasing the uptake and accumulation of nano-TiO$_2$ in daphnids[30].

Furthermore, there was a significant correlation between As and Ti content in daphnids ($P<0.01$; Table 1), which also indicated that nano-TiO$_2$ as a carrier increased

As concentrations in this organism. In addition, under the same nano-TiO$_2$ level, the correlation coefficients associated with the higher *As* exposure level (i.e., EC$_{50}$) were greater than those associated with the lower *As* exposure level (i.e., 75 μg/L; Table 1), demonstrating that the percentage of adsorbed *As* onto nano-TiO$_2$ under increasing *As* exposure levels progressively decreased, which in turn allowed for the ingestion and accumulation of a greater amount of free *As* in daphnids. Collectively, nano-TiO$_2$ was found to play a significant role as an *As*(III) carrier as well as its considerable accumulation in daphnids. Similarly, Tan et al.[31] found that daphnids increasingly ingested more Cd and zinc (Zn) as a result of their adsorption onto nano-TiO$_2$. Fan et al.[18] also showed that nano-TiO$_2$ increased the Cu accumulation in daphnids by 18–31% compared to the control. Zhang et al.[32] reported that nano-TiO$_2$ increased Cd concentrations in carp resulting from its adsorption onto nano-TiO$_2$, playing a Cd "carrying" role to daphnids. In addition, Sun et al.[33] also found that under 200 μg/L *As*(III) exposure, the addition of nano-TiO$_2$ increased *As* content in carp by 42–185.7% compared to the control.

In contrast, our current study found that the carrier role that nano-TiO$_2$ plays in *As*(III) transport weakened under increasing *As*(III) exposure treatments (Fig. 1). One reason for this was that greater *As* intake by daphnids was in the form of free ions that did not adsorb onto nano-TiO$_2$, weakening the carrier role that nano-TiO$_2$ plays on *As*(III) because the particulate reached beyond its maximum capacity in effecting *As*(III) adsorption under increasing *As*(III) exposure treatments. Another reason is that an increase in exposure *As*(III) levels could decrease the ingestive ability of daphnids under heightened *As*(III) stress, subsequently decreasing *As*(III) intake associated with nano-TiO$_2$ during laboratory culture.

3.3 Spatial and subcellular distribution

3.3.1 Spatial distribution

The spatial distribution of *As* and Ti in daphnids (Fig. 2 and 3, respectively) showed that nano-TiO$_2$ and *As* chiefly accumulated in the gut. Moreover, *As* in daphnids increased by a factor of 7 and Ti increased by a factor of 10, while nano-TiO$_2$ levels

increased from 2 mg/L to 20 mg/L, respectively. Specifically, the 75 μg/L *As*(III) exposure treatment under 2 mg/L and 20 mg/L nano-TiO$_2$ levels exhibited a significant correlation between *As* and Ti (*R*=0.656, *P*<0.01; *R*=0.801, *P*<0.01, respectively) in all daphnid samples (data not shown). In contrast, *As* was not significantly correlated to Ti (*P*>0.05) in part tissues of daphnids (excluding the guts). These findings further confirmed that nano-TiO$_2$ as a carrier can transport *As* into daphnid guts wherein they will almost exclusively accumulate.

3.3.2 Subcellular distribution

The subcellular distribution of *As* and Ti are shown in Fig. 4 and 5, respectively, namely, results after 6 and 24 h exposure under the 75 μg/L and EC$_{50}$ *As*(III) treatments along with the different nano-TiO$_2$ levels (i.e., 0, 2, 20 mg/L). When the *As*(III) exposure concentration was 75 μg/L (lower), most *As* was distributed into cellular debris and BDMs, which increased with increasing nano-TiO$_2$ levels. Moreover, accumulated *As* in MSFs decreased with increasing nano-TiO$_2$ levels (Fig. 4 A and B). Similarly, the accumulated Ti in BDMs and cellular debris was higher than the accumulated Ti in MSFs (Fig. 5 a and b). Moreover, we did not find any significant difference between the 6 h and 24 h exposure treatments associated with subcellular fractions (*P*>0.05). Under the 75 μg/L *As*(III) exposure treatment, the higher accumulated *As* and Ti concentrations we found in BDMs and cellular debris demonstrated that the toxic effects of *As*(III) associated with nano-TiO$_2$ were relatively low[23].

In contrast, for the EC$_{50}$ *As*(III) exposure treatment (higher), most *As* was also distributed within BDMs and cellular debris, which continued to increase with increasing nano-TiO$_2$ levels, while the *As* that accumulated in MSFs increased with increasing nano-TiO$_2$ levels (Fig. 4 C and D). Accordingly, we did not find a significant difference between the 6 h and 24 h subcellular fraction exposure treatments (*P*>0.05). Additionally, accumulated *As* in MSFs was higher than the 75 μg/L *As*(III) exposure treatment, which demonstrated the toxic effects caused by the higher *As*(III) exposure treatment (Fig. 4). Furthermore, accumulated Ti in daphnids

was lower than the 75 μg/L *As*(III) exposure treatment (Fig. 5 c and d), implying that higher toxicity levels reduced the active ingestion of nano-TiO$_2$ by daphnids. In turn, the reduction in nano-TiO$_2$ uptake under the higher *As*(III) exposure treatment decreased its role as an *As* carrier (and the ensuing accumulation of *As*) to daphnids (Fig. 1). Additionally, given that nano-TiO$_2$ plays a critical role as a carrier of *As*(III) to daphnids, most *As* accumulated in BDMs and cellular debris, which are considered detoxified fractions in daphnids (Fig. 4 and 5). This could explain why *As*(III) toxicity associated with nano-TiO$_2$ decreased with increasing nano-TiO$_2$ levels.

Furthermore, a similar *As* and Ti accumulation pattern was clearly shown between the 6 h and 24 h exposure (duration) treatments and between the 75 μg/L and EC$_{50}$ exposure (level) treatments, which mostly accumulated in BDMs and cellular debris in the form of detoxified fractions in daphnids (Fig. 4 and 5). Therefore, regardless of *As*(III) exposure time or exposure level, the subcellular distribution of *As*(III) can itself explain the toxicological reduction in daphnids resulting from *As*(III) stress associated with nano-TiO$_2$ compared to *As*(III) alone.

3.4 Efflux of arsenic and titanium dioxide nanoparticles

After 24-h efflux from daphnids, both *As* and Ti concentrations stabilized (Fig. 6). Additionally, nano-TiO$_2$ elimination from daphnids was more difficult than *As*. This was determined by the higher *As* efflux percentage compared to the corresponding Ti percentage (Table S2). Previous studies also demonstrated that nano-TiO$_2$ intake is more difficult to expel due to its attachment in daphnid guts[19]. After 24-h efflux, calculated *As* efflux rates were 4.028 μg/(g · h) for 2 mg/L nano-TiO$_2$, 2.598 μg/(g · h) for 20 mg/L nano-TiO$_2$, and 1.56 μg/(g · h) for 0 mg/L nano-TiO$_2$, while calculated Ti efflux rates were 0.2 μg/(g · h) for 2 mg/L nano-TiO$_2$ and 30.34 μg/(g · h) for 20 mg/L nano-TiO$_2$. It is noteworthy that the lower Ti efflux rate (for the 2 mg/L nano-TiO$_2$ level) also yielded the highest *As* efflux rate, which indicated that *As* dissociated from nano-TiO$_2$ in daphnid guts before being expelled in the form of free *As*[30]. Furthermore, according to their efflux percentage rates (Table S2), both the *As* and Ti efflux percentages decreased with increasing nano-TiO$_2$

levels, implying that elevated amounts of nano-TiO$_2$ yielded lower *As* efflux from daphnids. This demonstrated that nano-TiO$_2$ still sequesters some *As* in daphnids due to *As* adsorption onto this particulate, particularly under higher nano-TiO$_2$ exposure levels. Such immobilization by nano-TiO$_2$ could potentially result in higher *As* accumulation in daphnids, potentially resulting in health risks across the food chain. Direct and reproduction efflux were the two main efflux pathways that daphnids used to expel accumulated *As* and Ti, while molting only accounted for a small overall proportion (Fig. 7). Specifically, as a secondary efflux pathway, *As* and Ti reproduction efflux could potentially transfer accumulated *As* and Ti to the next generation when both *As*(III) and nano-TiO$_2$ are present[34], and particularly when *As*(III) is present alone.

3.5 Environmental implications

In this study, significant correlations between *As* and Ti concentrations in daphnids based on uptake data indicated that nano-TiO$_2$ as a carrier increased the intake of *As*(III) in daphnids. Moreover, according to the spatial distribution of *As* and Ti in daphnids, we found a significant correlation between *As* and Ti; however, we did not find a significant correlation in part tissue components (i.e., without guts). This further confirmed that nano-TiO$_2$ as a carrier can transport *As* into daphnid guts. Additionally, nano-TiO$_2$ was found to reduce *As*(III) toxicity in *D. magna*. Similar studies also proposed that nano-TiO$_2$ decreases *As* and Cu toxicity[17]. Our previous study demonstrated that nano-TiO$_2$ in test media had only limited toxic effects on *D. magna*[21]. In turn, *As*(III) toxicity associated with nano-TiO$_2$ was caused by *As*(III). Accordingly, nano-TiO$_2$ was able to rapidly adsorb *As*(III) to a state of equilibrium within 30 min, resulting in a decrease of free *As* during the water phase, subsequently reducing *As*(III) mobility in daphnids that could potentially cause toxic effects. Moreover, although *As* accumulation in daphnids was enhanced by the presence of nano-TiO$_2$ acting as a carrier, accumulated *As* located within the intestines and corresponding detoxified fractions, namely, BDMs and cellular debris, was distributed as an operational characteristic[21], consequently reducing *As*(III) toxicity associated

with nano-TiO$_2$. It is noteworthy that regardless of exposure time (i.e., 6 and 24 h) or exposure level of *As*(III) (i.e., 75 μg/L and EC$_{50}$), most *As* and Ti in daphnids accumulated in BDMs and cellular debris in the form of detoxified fractions. These observations supported that not matter with the exposed time and exposed levels of *As*(III), their reduced toxicity on daphnids could be explained by the subcellular distribution of *As* and Ti.

Changes in the intestinal environment (i.e., changes associated with *As* intestinal enzymes, microbes, pH, etc.) can cause *As*(III) to unequivocally dissociate from nano-TiO$_2$[15, 21]. *As* dissociation could result in increased mobility, causing *As* elimination by direct efflux and reproduction efflux. In particular, reproduction efflux (the secondary efflux pathway) of *As* and Ti could potentially transfer accumulated *As* and Ti to the next generation. Furthermore, the *As* efflux percentage decreased with increasing nano-TiO$_2$ levels, which implies that elevated nano-TiO$_2$ levels produce lower *As* efflux from daphnids. This will cause higher *As* accumulation in daphnids, which could potentially cause health risks across the food chain.

Furthermore, *As* accumulation could also alter *As*(III) speciation and its associative subcellular distribution, subsequently reducing corresponding *As*(III) toxicity in the presence of nano-TiO$_2$. In nature, *As* toxicity on daphnids in the presence of nano-TiO$_2$ is influenced by many environmental factors including their food sources and internal physiological processes. Moreover, the accumulated *As* in daphinids would be transferred across food chain, which threatens aquatic security even human health. Therefore, investigating *As*(III) toxicity on aquatic organisms is necessary and has important practical significance in the presence of nano-TiO$_2$.

4 Conclusions

Acting as a carrier, nano-TiO$_2$ increased *As*(III) accumulation in *D. magna*. This was supported by changes in *As* and Ti accumulation as well as the significant correlations in spatial distribution between these two elements in this daphnid species. However, nano-TiO$_2$ as a carrier of *As*(III) weakened owing to elevated toxicological

levels and its limited adsorption capacity onto nano-TiO$_2$ as exposure levels increased. Results from this study showed that nano-TiO$_2$ increased *As*(III) accumulation in *D. magna* but not its subsequent level of toxicity. Specifically, nano-TiO$_2$ decreased *As*(III) toxicity in *D. magna*. Furthermore, most *As* accumulated in BDMs and cellular debris, considered to be detoxified fractions in daphnids, and this could explain why *As*(III) toxicity associated with nano-TiO$_2$ decreased with increasing nano-TiO$_2$ levels. Additionally, regardless of exposure time or exposure level of *As*(III), the subcellular distribution of *As* explains the lower toxicity in daphnids resulting from *As*(III) stress associated with nano-TiO$_2$. It is noteworthy that higher nano-TiO$_2$ levels yielded lower *As* efflux from daphnids, which demonstrated that nano-TiO$_2$ still sequesters some *As* in daphnids due to *As* adsorption onto the particulate. Furthermore, direct efflux and reproduction efflux were the two main pathways used to expel accumulated *As* and Ti, while molting only accounted for a small overall proportion. Importantly, being the secondary efflux pathway, reproduction efflux of *As* and Ti could potentially transfer accumulated *As* and Ti to the next generation under the co-occurrence of *As*(III) and nano-TiO$_2$. Further research is necessary to investigate the bioavailability and toxicity of *As*(III) in the presence of nano-TiO$_2$ in conjunction with an algal food source, taking into account different environmental factors, longer exposure times, and the various algal species involved.

Conflicts of interest

There are no conflicts of interest to declare

Acknowledgments

1
2
3
4
5
6
7
8
9
10
11
12
13
14
15
16
17
18
19
20
21
22
23
24
25
26
27
28
29
30
31
32
33
34
35
36
37
38
39
40
41
42
43
44
45
46
47
48
49
50
51
52
53
54
55
56
57
58
59
60

Reference

1.   C. C. Kuo, K. A. Moon, S. L. Wang, E. Silbergeld and A. Navas-Acien, The Association of Arsenic Metabolism with Cancer, Cardiovascular Disease, and Diabetes: A Systematic Review of the Epidemiological Evidence, *Environ Health Persp*, 2017, 125: 087001.

2.   T. Luo, H. X. Tian, Z. Guo, G. Q. Zhuang and C. Y. Jing, Fate of Arsenate Adsorbed on Nano-TiO2 in the Presence of Sulfate Reducing Bacteria, *Environ. Sci. Technol.*, 2013, **47**, 10939-10946.

3.   E. Moreno-Jimenez, E. Esteban and J. M. Penalosa, The fate of arsenic in soil-plant systems, *REV ENVIRON CONTAM T*, 2012, **215**, 1-37.

4.   P. L. Smedley and D. G. Kinniburgh, A review of the source, behaviour and distribution of arsenic in natural waters, *Appl Geochem*, 2002, **17**, 517-568.

5.   Z. H. Wang, Z. X. Luo, C. Z. Yan and B. S. Xing, Impacts of environmental factors on arsenate biotransformation and release in Microcystis aeruginosa using the Taguchi experimental design approach, *Water Res*, 2017, **118**, 167-176.

6.   Z. Wang, H. Gui, Z. Luo, I. L. Sarakiotia, C. Yan and G. D. Laing, Arsenic release: Insights into appropriate disposal of arsenic-loaded algae precipitated from arsenic contaminated water, *J Hazard Mater*, 2019, **384**, 121249.

7.   S. K. T. Mandal B K, Arsenic round the world: a review, *Talanta*, 2002, **58**, 201-235.

8.   A. Rahman, C. Granberg and L. A. Persson, Early life arsenic exposure, infant and child growth, and morbidity: a systematic review, *ARCH TOXICOL*, 2017, **91**, 3459-3467.

9.   H. A. Michael, An Arsenic Forecast for China, *Science*, 2013, **341**, 852-853.

10.   P. L. Smedley, A review of the source, behaviour and distribution, *Appl Geochem*, 2002, **17**, 517-568.

11.   E. J. Cho, H. Holback, K. C. Liu, S. A. Abouelmagd, J. Park and Y. Yeo, Nanoparticle characterization: state of the art, challenges, and emerging technologies, *MOL PHARMACEUT*, 2013, **10**, 2093-2110.

12.   A. F. Aravantinou, V. Tsarpali, S. Dailianis and I. D. Manariotis, Effect of cultivation media on the toxicity of ZnO nanoparticles to freshwater and marine microalgae, *ECOTOX ENVIRON SAFE*, 2015, **114**, 109-116.

13.   A. A. Keller and A. Lazareva, Predicted Releases of Engineered Nanomaterials: From Global to Regional to Local, *ENVIRON SCI TECH LET*, 2014, **1**, 65-70.

14.   C. Tan and W. X. Wang, Modification of metal bioaccumulation and toxicity in Daphnia magna by titanium dioxide nanoparticles, *ENVIRON POLLUT*, 2014, **186**, 36-42.

15.   Z. Luo, Z. Wang, Y. Yan, J. Li, C. Yan and B. Xing, Titanium dioxide nanoparticles enhance inorganic arsenic bioavailability and methylation in two freshwater algae species, *Environ Pollut*, 2018, **238**, 631-637.

16.　　R. Deng, D. H. Lin, L. Z. Zhu, S. Majumdar, J. C. White, J. L. Gardea-Torresdey and B. S. Xing, Nanoparticle interactions with co-existing contaminants: joint toxicity, bioaccumulation and risk, *Nanotoxicology*, 2017, **11**, 591-612.

17.　　R. R. Rosenfeldt, F. Seitz, R. Schulz and M. Bundschuh, Heavy metal uptake and toxicity in the presence of titanium dioxide nanoparticles: a factorial approach using Daphnia magna, *Environ Sci Technol*, 2014, **48**, 6965-6972.

18.　　W. Fan, M. Cui, H. Liu, C. Wang, Z. Shi, C. Tan and X. Yang, Nano-TiO2 enhances the toxicity of copper in natural water to Daphnia magna, *Environ Pollut*, 2011, **159**, 729-734.

19.　　W. W. Yang, Y. Wang, B. Huang, N. X. Wang, Z. B. Wei, J. Luo, A. J. Miao and L. Y. Yang, TiO2 nanoparticles act as a carrier of Cd bioaccumulation in the ciliate Tetrahymena thermophila, *Environ Sci Technol*, 2014, **48**, 7568-7575.

20.　　C. Z. Yan, F. Yang, Z. S. Wang, Q. Q. Wang, F. Seitz and Z. X. Luo, Changes in arsenate bioaccumulation, subcellular distribution, depuration, and toxicity in Artemia salina nauplii in the presence of titanium dioxide nanoparticles, *Environ Sci-Nano*, 2017, **4**, 1365-1376.

21.　　M. Li, Z. Luo, Y. Yan, Z. Wang, Q. Chi, C. Yan and B. Xing, Arsenate Accumulation, Distribution, and Toxicity Associated with Titanium Dioxide Nanoparticles in Daphnia magna, *Environ Sci Technol*, 2016, **50**, 9636-9643.

22.　　P. L. Klerks and P. R. Bartholomew, Cadmium Accumulation and Detoxification in a Cd-Resistant Population of the Oligochaete Limnodrilus-Hoffmeisteri, *AQUAT TOXICOL*, 1991, **19**, 97-112.

23.　　W. G. Wallace, B. G. Lee and S. N. Luoma, Subcellular compartmentalization of Cd and Zn in two bivalves. I. Significance of metal-sensitive fractions (MSF) and biologically detoxified metal (BDM), *Mar Ecol Prog Ser*, 2003, **249**, 183-197.

24.　　D. W. Engel, Accumulation and cytosolic partitioning of metals in the American oyster Crassostrea virginica, *MAR ENVIRON RES*, 1999, **47**, 89-102.

25.　　W. X. Wang and L. D. Guo, Influences of natural colloids on metal bioavailability to two marine bivalves, *Environ Sci Technol*, 2000, **34**, 4571-4576.

26.　　Z. Luo, M. Li, Z. Wang, J. Li, J. Guo, R. R. Rosenfeldt, F. Seitz and C. Yan, Effect of titanium dioxide nanoparticles on the accumulation and distribution of arsenate in Daphnia magna in the presence of an algal food, *ENVIRON SCI POLLUT R*, 2018, **25**, 20911-20919.

27.　　P. K. Dutta, A. K. Ray, V. K. Sharma and F. J. Millero, Adsorption of arsenate and arsenite on titanium dioxide suspensions, *J COLLOID INTERF SCI*, 2004, **278**, 270-275.

28.　　D. Nabi, I. Aslam and I. A. Qazi, Evaluation of the adsorption potential of titanium dioxide nanoparticles for arsenic removal, *Journal of Environmental Sciences*, 2009, **21**, 402-408.

29.　　x. g. M. Maria pena, geoge P.Korfiatis, Adsorption Mechanism of Arsenic, *Environ.Sci.Technol.*, 2006, **40**, 1257-1262.

30.　　L. Y. Tan, B. Huang, S. Xu, Z. B. Wei, L. Y. Yang and A. J. Miao, Aggregation Reverses the Carrier Effects of TiO2 Nanoparticles on Cadmium Accumulation in the Waterflea Daphnia magna, *Environ. Sci. Technol.*, 2017, **51**, 932-939.

31.　　C. Tan, W. H. Fan and W. X. Wang, Role of titanium dioxide nanoparticles in the elevated uptake and retention of cadmium and zinc in Daphnia magna, *Environ Sci Technol*, 2012, **46**, 469-476.

32.　　X. Zhang, H. Sun, Z. Zhang, Q. Niu, Y. Chen and J. C. Crittenden, Enhanced bioaccumulation of cadmium in carp in the presence of titanium dioxide nanoparticles, *Chemosphere*, 2007, **67**,

160-166.

33.   H. Sun, X. Zhang, Q. Niu, Y. Chen and J. C. Crittenden, Enhanced Accumulation of Arsenate in Carp in the Presence of Titanium Dioxide Nanoparticles, *Water, Air, and Soil Pollution*, 2006, **178**, 245-254.

34.   D. J. H. Phillips, Metabolic pathways involving arsenic in marine organisms: A unifying hypothesis, *MAR ENVIRON RES*, 1985, **17**, 1-12.

Figures captions

Fig. 1 Arsenic (*As*; A and B) and titanium (Ti; C and D) contents in *Daphnia magna* exposed to *As*(III) treatments of 75 μg/L (A and C) and EC_{50} (B and D) under different nano-TiO_2 levels (0, 2, and 20 mg/L).

Fig. 2 Spatial distribution of arsenic (As) and titanium (Ti) in *Daphnia magna* exposed to 75 μg/L arsenite associated with 2 mg/L nano-TiO_2. A and B represent whole dephnids, while C and D represent part tissue of daphnids (excluding the guts).

Fig. 3 Spatial distribution of arsenic (*As*) and titanium (Ti) in *Daphnia magna* exposed to 75 μg/L arsenite associated with 20 mg/L nano-TiO_2. A and B represent whole dephnids, while C and D represent part tissue of daphnids (excluding the guts)

Fig. 4 Arsenic (*As*) concentrations in biologically detoxified metals (BDM), cellular debris, and metal-sensitive fractions (MSF) at exposure treatments of 75 μg/L *As*(III) for 6 h (A) and 24 h (B), and EC_{50} *As*(III) for 6 h (C) and 24 h (D) associated with three different nano-TiO_2 levels.

Fig. 5 Titanium (Ti) concentrations in biologically detoxified metals (BDM), cellular debris, and metal-sensitive fractions (MSF) at exposure treatments of 75 μg/L *As*(III) for 6 h (A) and 24 h (B), and EC_{50} As(III) for 6 h (C) and 24 h (D) associated with three different nano-TiO_2 levels.

Fig. 6 Changes in arsenic and titanium contents in *Daphnia magna* during metabolic elimination under the treatments of 75 μg/L of *As*(III) with three different nano-TiO_2 levels.

Fig. 7 Metabolized arsenic (As) and titanium (Ti) concentrations in *Daphnia magna* through direct efflux, reproductive efflux, and metabolic molting under exposure 75 μg/L of *As*(III) associated with three different nano-TiO_2 concentrations

Fig. S1 Scanning electron microscope (SEM) images of nano-TiO_2 dispersal in (a) ultrapure water and (b) simplified Elendt M7 medium (SM7).

Fig. S2 Arsenite adsorption onto 2 and 20 mg/L of nano-TiO$_2$.

1
2
3
4
5
6

Figures

7
8
9
10
11
12
13
14
15
16
17
18
19
20
21
22
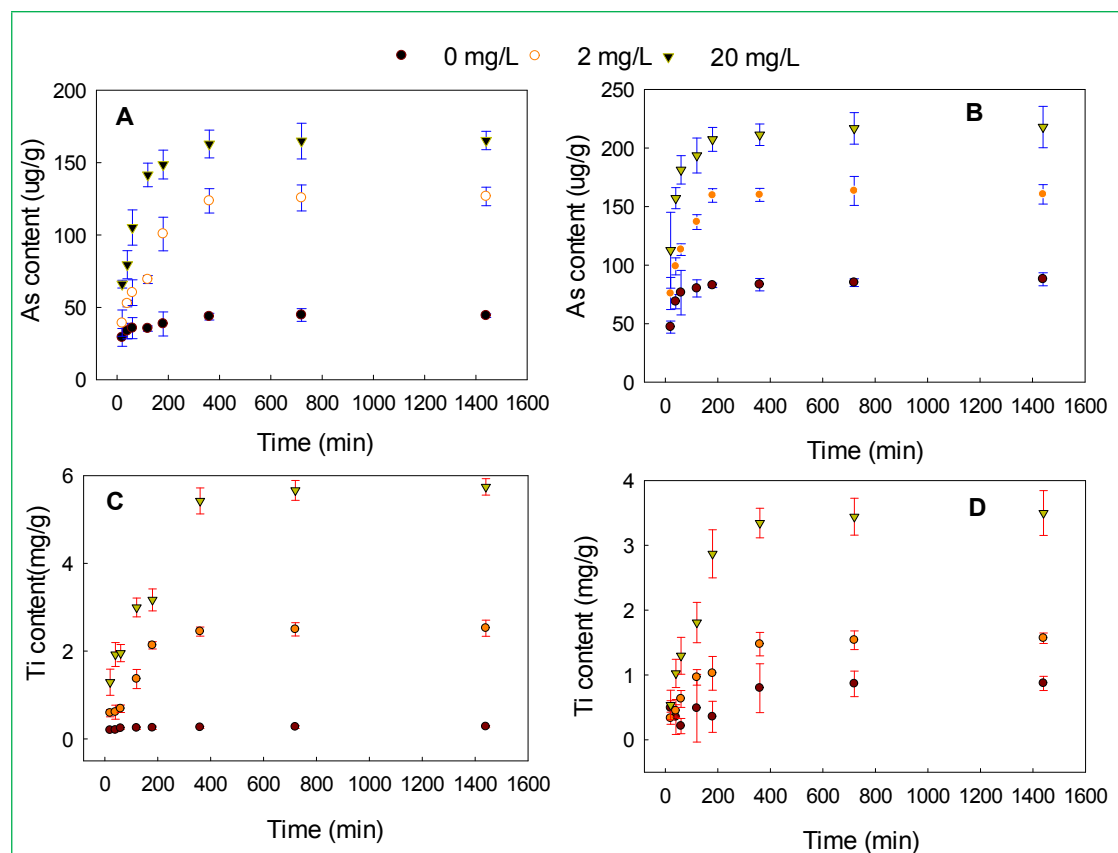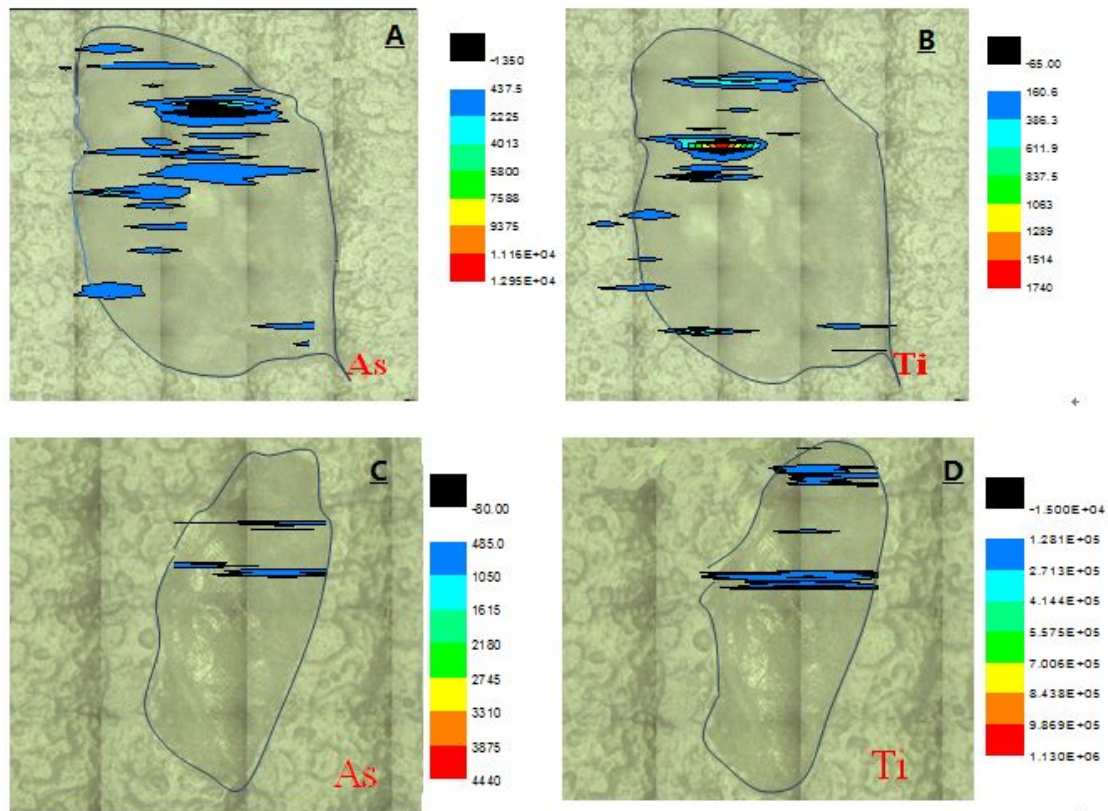23
24
25
26
27
28
29
30
31
32
33
34

35
36
37
38
39
40

Fig. 1 Arsenic (*As*; A and B) and titanium (Ti; C and D) contents in *Daphnia magna* exposed to *As*(III) treatments of 75 μg/L (A and C) and EC_{50} (B and D) under different nano-TiO$_2$ levels (0, 2, and 20 mg/L).

41
42
43
44
45
46
47
48
49
50
51
52
53
54
55
56
57
58
59
60

Fig. 2 Spatial distribution of arsenic (*As*) and titanium (Ti) in *Daphnia magna* exposed to 75 μg/L arsenite associated with 2 mg/L nano-TiO$_2$. A and B represent whole dephnids, while C and D represent part tissue of daphnids (excluding the guts).
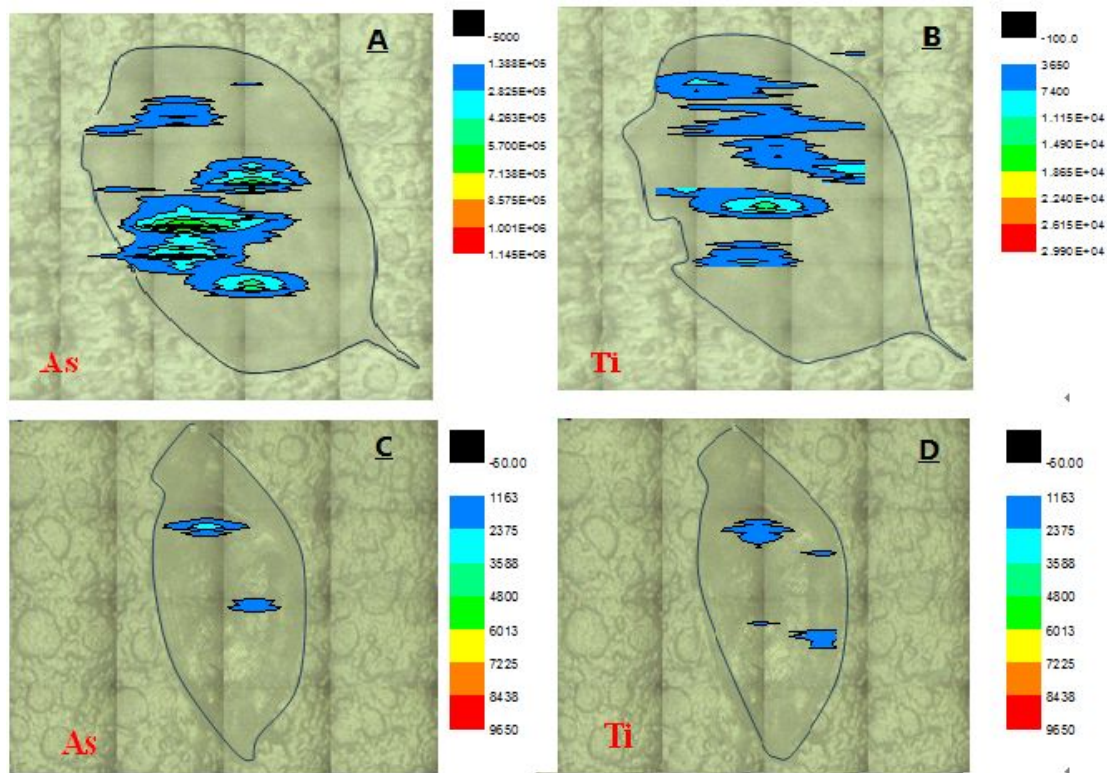
Fig. 3 Spatial distribution of arsenic (*As*) and titanium (Ti) in *Daphnia magna* exposed to 75 μg/L arsenite associated with 20 mg/L nano-TiO$_2$. A and B represent whole dephnids, while C and D represent part tissue of daphnids (excluding the guts)
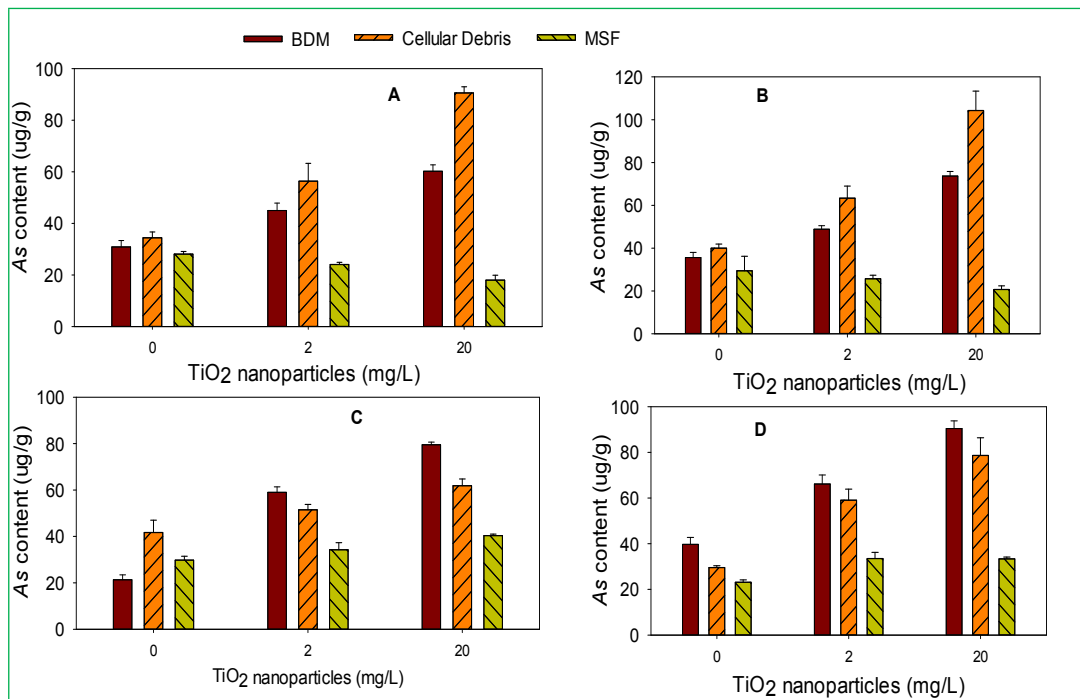
Fig. 4 Arsenic (*As*) concentrations in biologically detoxified metals (BDM), cellular debris, and metal-sensitive fractions (MSF) at exposure treatments of 75 μg/L *As*(III) for 6 h (A) and 24 h (B), and EC_{50} *As*(III) for 6 h (C) and 24 h (D) associated with three different nano-TiO_2 levels.
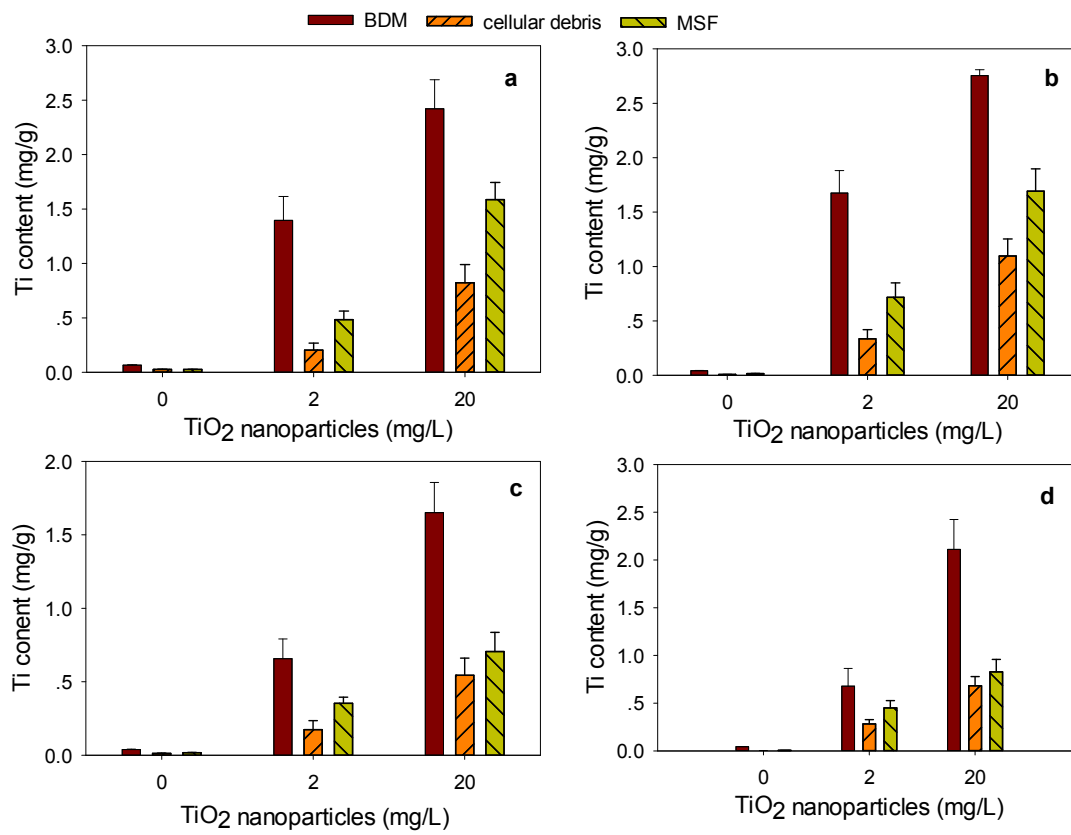
Fig. 5 Titanium (Ti) concentrations in biologically detoxified metals (BDM), cellular debris, and metal-sensitive fractions (MSF) at exposure treatments of 75 μg/L *As*(III) for 6 h (A) and 24 h (B), and EC_{50} As(III) for 6 h (C) and 24 h (D) associated with three different nano-TiO$_2$ levels.
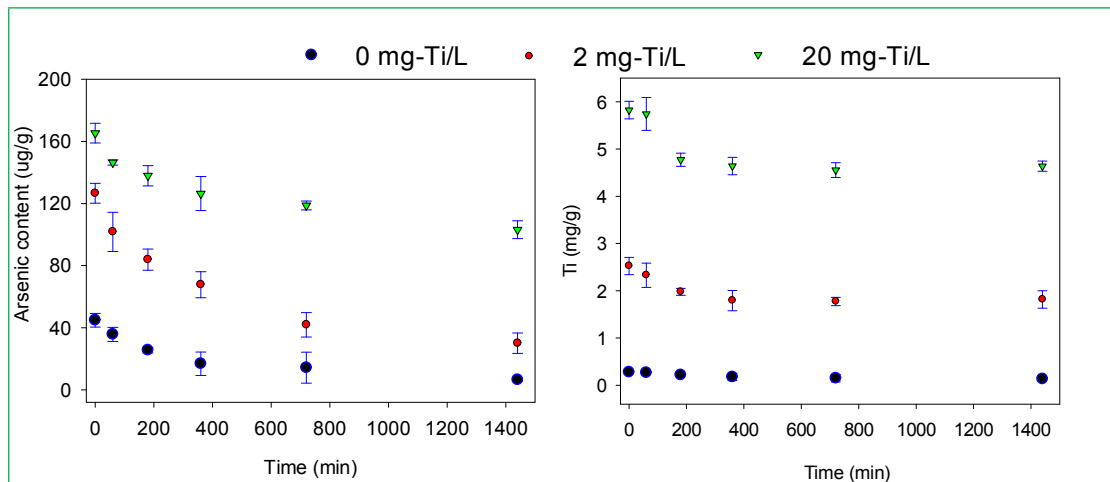
Fig. 6 Changes in arsenic and titanium contents in *Daphnia magna* during metabolic elimination under the treatments of 75 μg/L of *As*(III) with three different nano-TiO$_2$ levels.
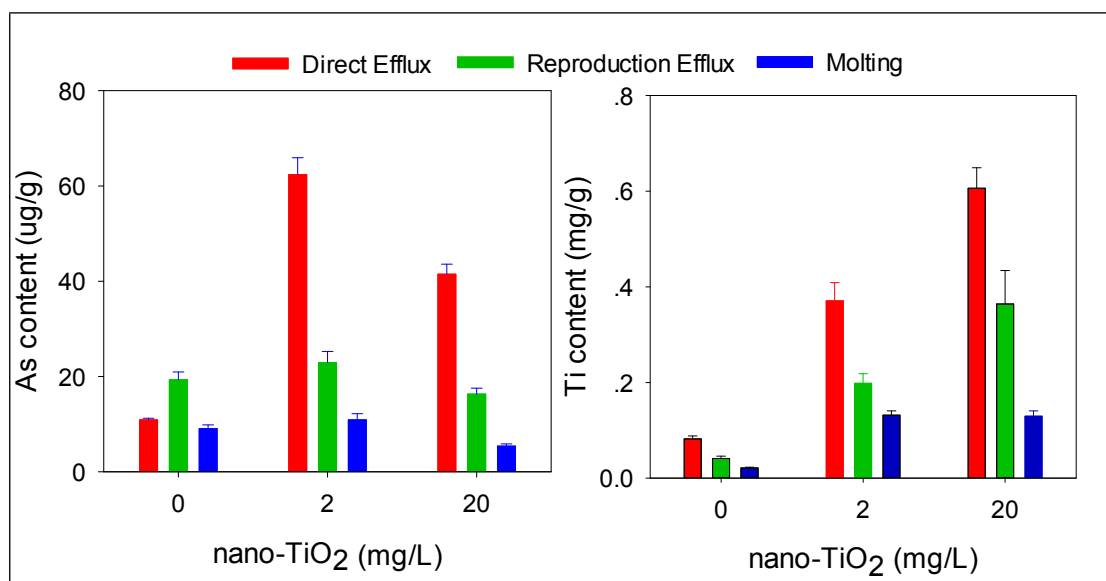
Fig. 7 Metabolized arsenic (As) and titanium (Ti) concentrations in *Daphnia magna* through direct efflux, reproduction efflux, and metabolic molting under exposure 75 μg/L of *As*(III) associated with three different nano-TiO$_2$ concentrations

Tables

Table 1 Relationship between arsenic (*As*) and titanium (Ti) contents in *Daphnia magna* for the different nano-TiO$_2$ exposure levels and arsenite concentrations under 75 μg/L and EC$_{50}$ exposure level treatments.

As(III) exposure level	Ti (2 mg/L nano-TiO$_2$)	Ti (20 mg/L nano-TiO$_2$)
As (75 μg/L)	0.982**	0.970**
As (EC$_{50}$)	0.936**	0.911**

** indicates *P*<0. 01

Graphical abstract

This study provided new insights into the "Trojan horse" effects of nano-TiO$_2$ on arsenite (*As*(III)) bioaccumulation in *Daphnia magna*.